PAPER

The effect of donor-modification in organic light-harvesting motifs: triphenylamine donors appended with polymerisable thienyl subunits†

Catherine Bonnier,[a] Devin D. Machin,[a] Omar K. Abdi,[a] Kiyoshi C. D. Robson[b] and Bryan D. Koivisto*[a]

A family of seven organic triphenylamine-based dyes suitable for dye-sensitized solar cell (DSSC) applications is reported. The donor portion of these dyes has been systematically modified using polymerisable thienyl subunits. The physicochemical properties and device performance are discussed with device efficiencies ranging from 5.51 to 6.65%.

Introduction

While dye-sensitized solar cells (DSSCs) have attracted growing interest because of their ease of fabrication and low cost, there are still significant problems with the commonly employed I^-/I_3^- liquid electrolyte,[1] namely, the I^-/I_3^- electrolyte corrodes metal contacts and electrodes; I_3^- partially absorbs visible light;[2] the electrolyte itself photodegrades; the presence of small amounts of I_2 can interact with or decompose the dye[3] and because of the volatile nature of the electrolyte solution only finite temperature ranges may be tolerated for cell operation. These limitations are partially responsible for long-term stability and performance issues and ultimately limits the widespread applicability of DSSCs. To avoid these problems a new electrolyte is required. Recent studies have focused on alternative redox couples,[2,4] ionic liquids,[5] and solid-state[6] or polymer hole transport materials[7] (HTM). Polymer-based HTMs are particularly attractive due to their rapid hole mobility, and polyethylenedioxythiophene (PEDOT) has been shown to be an effective HTM in DSSCs.[7,8]

Concomitantly, organic-based photosensitizers have become increasingly popular for light-harvesting applications owing to an improved understanding of the requisite structure–property relationships.[9] For example, all organic dyes for DSSC applications are comprised of a redox-active donor/chromophore (D) that is coupled through a π-conjugated spacer to an acceptor (A) capable of anchoring to TiO_2.[9,10]

Furthermore, there have been an increasing number of examples that suggest that organic dyes can be systematically tuned[11,12] to have improved interactions with I^-/I_3^-, and in many cases can outperform their ruthenium-based counterparts when using novel electrolytes.[4,7,8]

While a great deal of synthetic effort has been put into developing unique π-spacers capable of increasing charge separation and bathochromically shifting the absorption profile,[13,14] the modification of the redox-active donor with electron-rich π-systems has been less studied.[15–17] Triphenylamines (TPAs) are the most commonly employed donors in organic motifs because of their intense absorption and rich redox behaviour.[18]

Our motivation for this work began with a report by Liu and Ramakrishna, where they found that an indoline-based dye could effectively sensitize TiO_2, and outperform Z907, when using polyEDOT as an HTM (*in situ* polymerization of EDOT using photochemical or electrochemical methods).[7] In that report they observed a titania thickness dependence on device performance, and suggested that the nature of the sensitizer could affect the effective penetration depth of the polymer HTM.

We wanted to systematically study this hypothesis and propose that if a donor, like the TPA in the previously reported **1**,[19] is equipped with polymerizable subunits, the resulting family of dyes may be able to integrate with the polymer film leading to increased pore filling, decreased dye–HTM interfacial capacitance, minimized recombination and improved long term stability. To this end, we have prepared a family of dyes based on **1** where the TPA donor is functionalized with pendant thiophene arms that are conjugated to the donor. Before exploring these dyes in HTM-based devices, we have examined the effect of donor modification on the physicochemical properties and device performance with the traditional I^-/I_3^- electrolyte. The results of this benchmark study are reported herein.

[a]*Department of Chemistry and Biology and the Centre for Urban Energy (CUE) Ryerson University, 350 Victoria St. Toronto, Ontario, Canada M5B 2K3. E-mail: bryan.koivisto@ryerson.ca; Fax: +1-416-979-5044; Tel: +1-416-979-5000 ext 4625*
[b]*Department of Chemistry, University of Calgary, Calgary, AB, Canada*

†Electronic supplementary information (ESI) available: Experimental data and characterization is available. See DOI: 10.1039/c3ob41288a

This journal is © The Royal Society of Chemistry 2013

Org. Biomol. Chem., 2013, **11**, 7011–7015 | **7011**

Synthesis

In order to examine the effect of TPA donor modification, we prepared a series of mono- and di-substituted thienyl derivatives (Fig. 1). As depicted in Schemes 1 and 2, the TPA donor is particularly well suited for this modification, because it can be readily equipped with pendant thiophene substituents. In Scheme 1, **2a**[20] and **2b**[21] serve as the starting points for Suzuki coupling with either 2- or 3-substituted thienyl boronic esters/ acids. After Suzuki coupling and a Knoevenagel condensation with cyanoacetic acid, dye families **4** and **8** were obtained in good yields (see ESI†). In the case of **6b**, bromination of **3b** led to aldehyde **5** which smoothly underwent a Knoevenagel

condensation with cyanoacetic acid to produce the desired di-substituted brominated TPA dye. Our impetus for brominating our dyes is to allow for postmodification and ideally facilitate polymerization with the HTM. Our current methodology precluded the possibility of preparing **6a**. The preparation of the conformationally more flexible family **12** used similar synthetic manipulations, but required a protection/deprotection methodology and the Horner–Wadsworth–Emmons reaction to ensure a *trans*-substituted olefin (Scheme 2).

Results and discussion

Electrochemical data and UV-Vis absorption data in DCM for the dyes and benchmark compound **1** have been presented in Table 1. All dyes exhibit a single reversible one electron oxidation. This is assigned as the HOMO energy, and is consistent with TPA oxidation.[14] The TPA unit is sensitive to donor modifications. Thienyl arms destabilize the HOMO, but the donating effect of substituted thiophenes varies according to the electron density arguments pertaining to thiophene rings. As can be observed in Table 1, a 2-substituted thiophene stabilizes the HOMO (∼30 mV) more than a 3-substituted thiophene (∼10 mV), owing to the higher electron density at the 2-position. The olefin substituted derivative, however, stabilizes the TPA HOMO owing to the increased s-character of the olefin substituent. Bromination stabilizes the HOMO (by ∼40 mV) when **6b** is compared to the non-brominated **4b**, because of the electron withdrawing nature of the halide. Finally, disubstitution enhances all of the electronic trends discussed above.

For all dyes, with the exception of **1**, sweeps to higher potential (∼1.3 V), beyond the reversible TPA oxidation, resulted in a pseudo reversible wave that grows in intensity
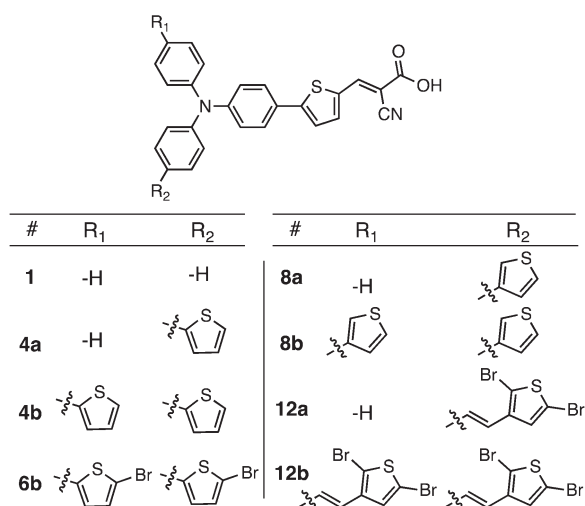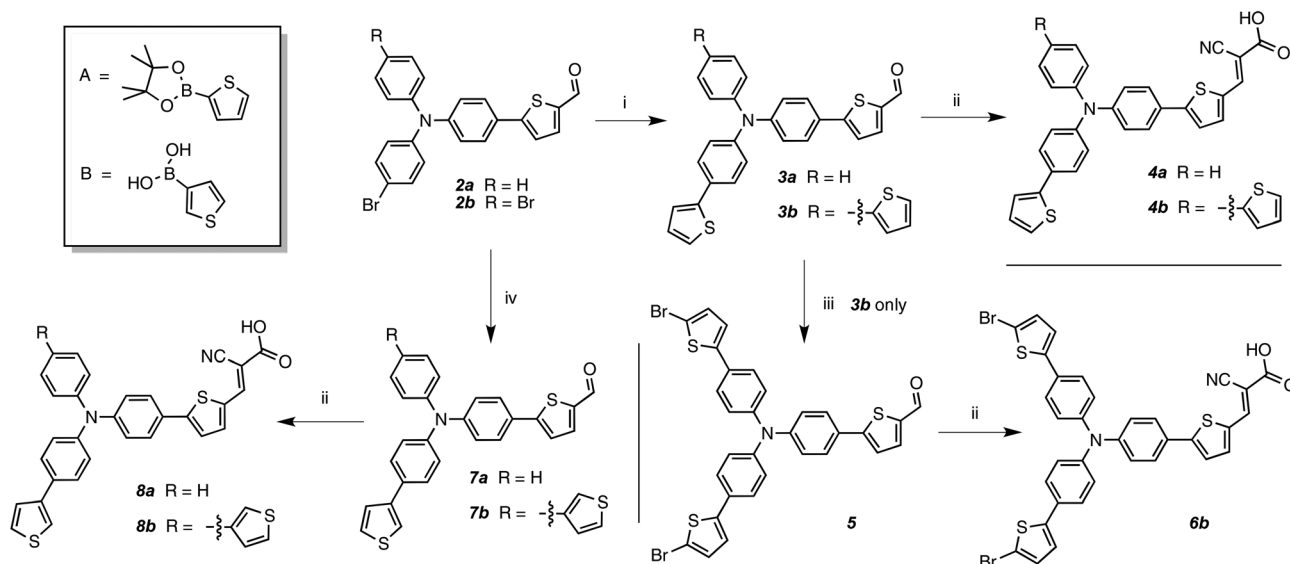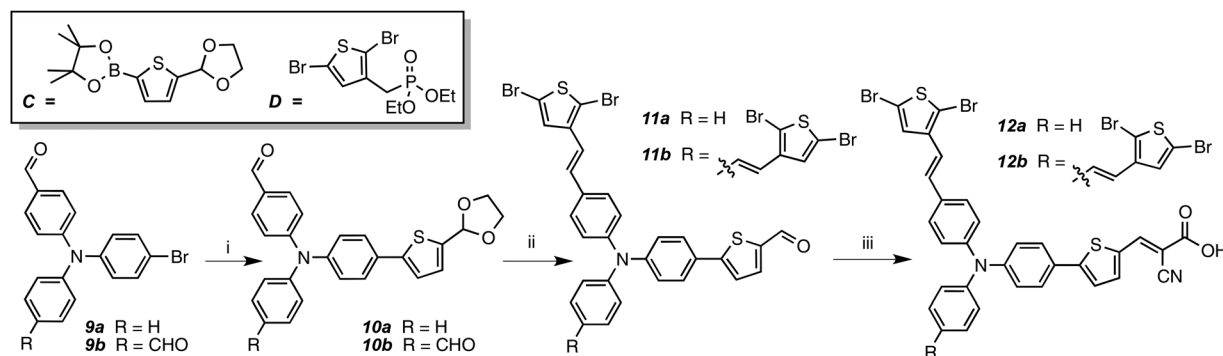

Fig. 1 A family of TPA dyes where the donor is substituted with various thienyl-subunits.

Scheme 1 Synthesis of dye families **4a**, **4b**,[22] **6b**, **8a** and **8b**. Reaction conditions: (i) A (1.15 or 2.3 eq.), K$_2$CO$_3$ (5 or 10 eq.), Pd(PPh$_3$)$_4$ (10 or 20 mol%), THF–H$_2$O 9 : 1, reflux 12 h; (ii) cyanoacetic acid (2 eq.), piperidine (0.25 eq.), CHCl$_3$, reflux 12 h; (iii) NBS (2.2 eq.), THF–EtOAc 1 : 1, 25 °C, 12 h; (iv) B (1.15 or 2.3 eq.), K$_2$CO$_3$ (5 or 10 eq.), Pd(PPh$_3$)$_4$ (10 or 20 mol%), THF–H$_2$O 9 : 1, reflux 12 h.

7012 | *Org. Biomol. Chem.*, 2013, **11**, 7011–7015

This journal is © The Royal Society of Chemistry 2013

Scheme 2 Synthesis of dye family **12**. Reaction conditions: (i) C (1.x eq.), K$_2$CO$_3$ (5 eq.), Pd(PPh$_3$)$_4$ (10 mol%), THF–H$_2$O 9 : 1, reflux 12 h; (ii) D (1.x or 2.x eq.), tBuOK (1.x or 2.x eq.), THF, reflux 24 h, glacial AcOH–H$_2$O 2 : 1, reflux, 1 h; (iii) cyanoacetic acid (2 eq.), piperidine (0.25 eq.), CHCl$_3$, reflux 12 h.

Table 1 Electrochemical and UV-Vis absorption data for dyes

Compound	$E_{1/2}$ (V vs. NHE)[a] TPA[•+]/TPA	UV-Vis[b] λ_{max}/nm ($\varepsilon \times 10^3$/M^{-1} cm^{-1})
1	1.27	479 (22.1), 346 (12.3)
4a	1.24	487 (37.4), 350 (30.6)
4b	1.21	492 (37.3), 360 (45.6)
6b	1.25	489 (39.3), 369 (54.2)
8a	1.26	487 (32.3), 329 (25.6)
8b	1.23	492 (33.9), 340 (37.6)
12a	1.29	486 (36.8), 371 (38.8)
12b	1.32	491 (33.9), 389 (53.8)

[a] Data collected using 0.1 M NBu$_4$PF$_6$ DCM solutions at 100 mV s^{-1} and referenced to a [Fc]/[Fc]$^+$ internal standard followed by conversion to NHE; [Fc]/[Fc$^+$] = +765 mV vs. NHE in DCM. [b] Data collected in DCM solutions.
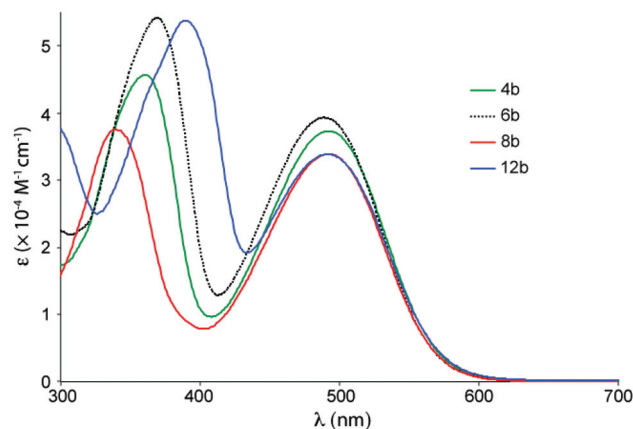

Fig. 2 UV-Vis spectra in DCM for the di-substituted TPA dyes.

with multiple scans. This observation suggests thiophene polymer formation at the electrode surface and is consistent with the formation of thiophene–TPA linkages.[23] An examination of the working electrode surface (ESI; Fig. S1†) after multiple scans shows the formation of an insoluble red polymeric film, which further supports the notion that these dyes could be successfully integrated with an HTM during an *in situ* polymerization.

A representative set of UV-Vis spectra recorded in DCM for **4b**, **6b**, **8b**, and **12b** are presented in Fig. 2 and tabulated in Table 1 (UV-Vis profiles of dyes **1**, **4a**, **8a**, and **12a** can be found in Fig. S2†). The UV-Vis spectra of all dyes show two significant absorptions: one at high energy and one at low energy centred at *ca.* 500 nm. When compared to the benchmark dye **1**, it was satisfyingly observed that modifying the TPA donor increased the extinction coefficients and moderately redshifted the low energy absorption envelope. The low energy absorption has been assigned as the HOMO–LUMO transition and DFT calculated (B3LYP/6-31G) frontier orbitals are presented in Fig. 3. However, the most significant differences due to modification of the TPA are observed in the high energy transition which has been assigned as the HOMO–LUMO + 1 transition.

The HOMO of these dyes is centred on the TPA, but delocalized over the entire molecule (Fig. 3). As a result of an increased optical cross-section, larger extinction coefficients

are observed. The LUMO is appropriately located on the cyano-acetic anchor in all cases. The LUMO + 1 is primarily localized on the polymerizable subunits. When the conjugation lengths between the TPA and thienyl-subunit are increased, a significant bathochromic shift is observed in the higher energy absorption. A similar trend is observed for the mono-substituted TPA derivatives (**4a**, **8a**, and **12a**); however, this high energy band is less intense in all mono-substituted derivatives.

With a detailed understanding of the physicochemical properties in solution, DSSC device performance was examined for our new family of dyes. The relevant parameters were extracted from the measured current–voltage traces under standard AM 1.5 sunlight and are detailed in Table 2. We were satisfied to observe that each of our modified dyes had a higher device efficiency than the benchmark dye **1**. The highest performing dyes were **4b** and **8b**, but surprisingly, **12b** had the lowest performance of this new family.

Several structure–property relationships can be observed in this series. The first is that disubstituted TPAs outperform mono-substituted derivatives owing to increased light harvesting (see Table 1). Furthermore, within the error of the measurement, there is no significant difference between 2- and 3-substituted thiophenes. **12a** and **12b**, with the olefin spacer,
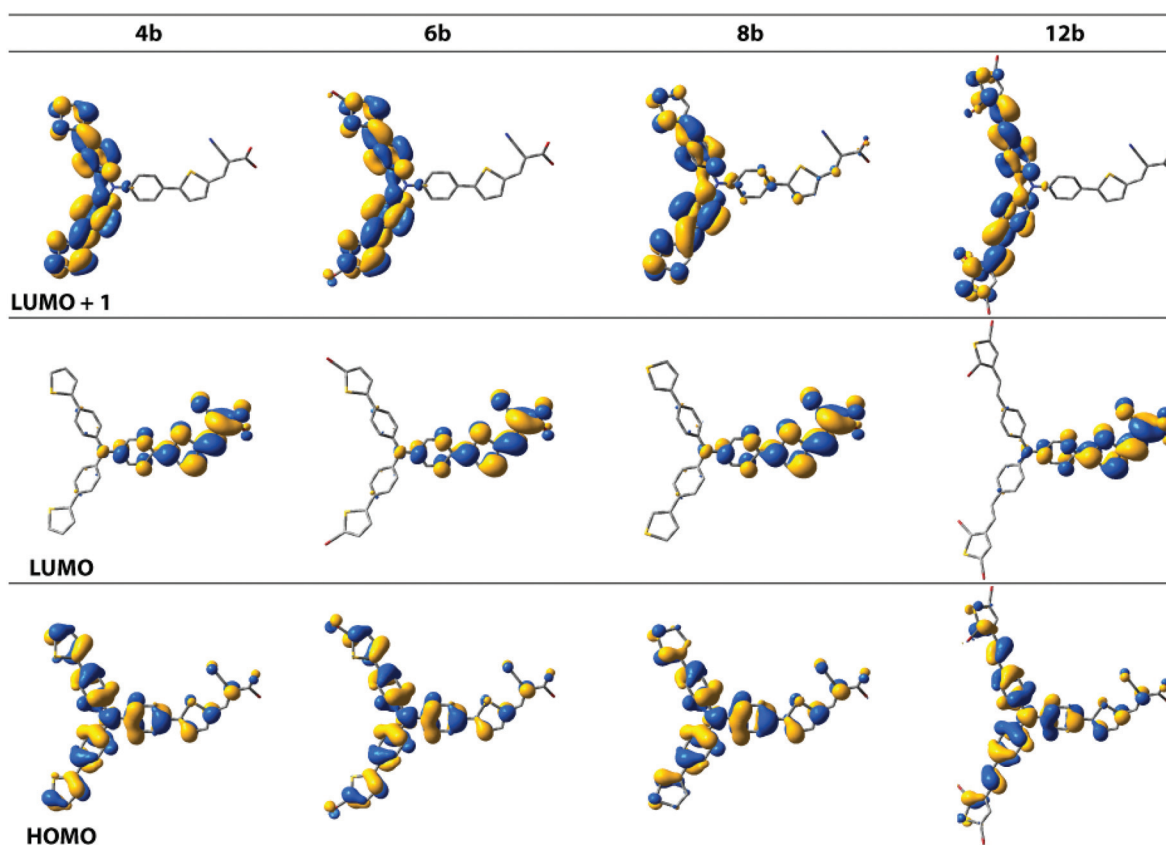
This journal is © The Royal Society of Chemistry 2013

Org. Biomol. Chem., 2013, **11**, 7011–7015 | **7013**

Fig. 3 Frontier molecular orbitals as predicted by DFT (B3LYP/6-31G) for di-substituted dyes **4b**, **6b**, **8b**, **12b**.

Table 2 Solar cell performance parameters obtained under simulated AM 1.5 illumination for select dyes[a]

Compound	J_{sc} (mA cm^{-2})	V_{oc} (V)	FF	η (%)
1	10.93	0.68	0.70	5.15
4a	11.65	0.70	0.72	5.84
4b	12.59	0.71	0.73	6.48
6b	12.12	0.71	0.72	6.23
8a	11.90	0.69	0.71	5.89
8b	12.86	0.71	0.72	6.56
12a	10.80	0.70	0.74	5.59
12b	11.33	0.68	0.72	5.51

[a] Device fabrication and data collection procedures can be found in the ESI.

were designed to offer conformational flexibility for future *in situ* polymerizations; therefore, it was a little disappointing to see this dye with the lowest performance. While differing dye–electrolyte interactions cannot be ruled out, all dyes were studied using the same **Z1137** I^-/I_3^- electrolyte and it is reasonable to assume that because these dyes have similar hydrophobicity, owing to their similar polyaromatic structure, regeneration mechanisms would not be rate limiting. Furthermore, assuming that we are operating within a normal Markus region, regeneration for **12b** should be fastest because it has the most stabilized HOMO. Heavy atom quenching (by the

bromine atoms) of the excited state can also be ruled out because the same poor performance was not observed in **6b**.

The incident photon-to-electricity conversion efficiency (IPCE) spectrum for disubstituted dyes is presented in Fig. 4. Despite having a similar profile to **4b** and **8b**, the current response for **12b** is ~10% lower for most of the visible spectrum.
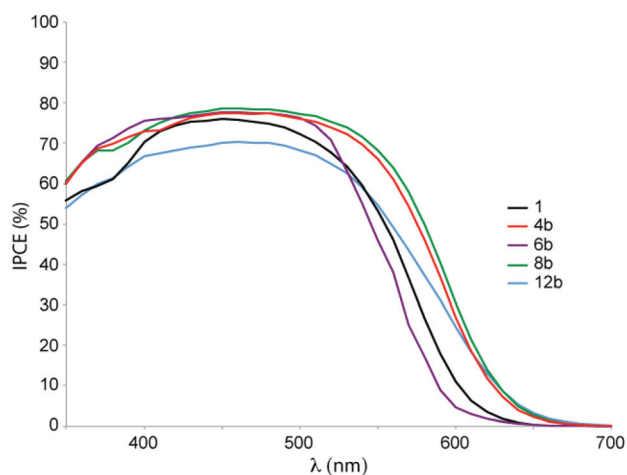

Fig. 4 Photocurrent action spectrum obtained for di-substituted dyes attached to TiO$_2$ films using the Z1137 electrolyte.

When considering the hydrodynamic volume of **12b**, the most rational explanation for the low J_{sc} and V_{oc} (and ultimately performance) is a reduced dye loading on the TiO$_2$ surface. Unfortunately, the preprogrammed conformational flexibility meant to facilitate integration with the HTM would also prohibit dye loading, once again reaffirming the classical organic reasoning that both electronics and sterics are important considerations in molecular design.

Conclusions

To gain a fundamental understanding of how donor modification can affect the physicochemical properties and device performance we have prepared a family of TPA dyes equipped with thienyl subunits. All dyes outperformed the benchmark dye **1** in device measurements owing to their improved photocurrents. These dyes show excellent promise for integration into polythiophene-based HTMs and we have demonstrated that the level of covalent bonding with the HTM could be varied through TPA modification (either mono- or di-substitution). This intimate connection with the HTM should facilitate hole-transport away from the dye rapidly stabilizing the photo-oxidized dye. Now that the I$^-$/I$_3^-$ electrolyte benchmark has been established we are poised to examine these dyes with HTM-based electrolytes. Studies are underway to examine the performance of these dyes in HTM–DSSC architectures and these results will be published in a future report.

Acknowledgements

Notes and references

1 G. Boschloo and A. Hagfeldt, *Acc. Chem. Res.*, 2009, **42**, 1819–1826.

2 M. Wang, N. Chamberland, L. Breau, J.-E. Moser, R. Humphry-Baker, B. Marsan, S. M. Zakeeruddin and M. Graetzel, *Nat. Chem.*, 2010, **2**, 385–389.

3 T. Marinado, K. Nonomura, J. Nissfolk, M. K. Karlsson, D. P. Hagberg, L. C. Sun, S. Mori and A. Hagfeldt, *Langmuir*, 2010, **26**, 2592–2598.

4 T. Daeneke, T.-H. Kwon, A. B. Holmes, N. W. Duffy, U. Bach and L. Spiccia, *Nat. Chem.*, 2011, **3**, 211–215.

5 V. Armel, J. M. Pringle, M. Forsyth, D. R. MacFarlane, D. L. Officer and P. Wagner, *Chem. Commun.*, 2010, **46**, 3146–3148.

6 I. Chung, B. Lee, J. He, R. P. H. Chang and M. G. Kanatzidis, *Nature*, 2012, **485**, 486–U494.

7 X. Liu, W. Zhang, S. Uchida, L. Cai, B. Liu and S. Ramakrishna, *Adv. Mater.*, 2010, **22**, E150–E155.

8 S. Yanagida, Y. Yu and K. Manseki, *Acc. Chem. Res.*, 2009, **42**, 1827–1838.

9 A. Mishra, M. K. R. Fischer and P. Bauerle, *Angew. Chem., Int. Ed.*, 2009, **48**, 2474–2499.

10 A. Hagfeldt, G. Boschloo, L. Sun, L. Kloo and H. Pettersson, *Chem. Rev.*, 2010, **110**, 6595–6663.

11 K. Hu, K. C. D. Robson, P. G. Johansson, C. P. Berlinguette and G. J. Meyer, *J. Am. Chem. Soc.*, 2012, **134**, 8352–8355.

12 K. C. D. Robson, K. Hu, G. J. Meyer and C. P. Berlinguette, *J. Am. Chem. Soc.*, 2013, **135**, 1961–1971.

13 W. D. Zeng, Y. M. Cao, Y. Bai, Y. H. Wang, Y. S. Shi, M. Zhang, F. F. Wang, C. Y. Pan and P. Wang, *Chem. Mater.*, 2010, **22**, 1915–1925.

14 C. Bonnier, D. D. Machin, O. Abdi and B. D. Koivisto, *Org. Biomol. Chem.*, 2013, **11**, 3756–3760.

15 C. Sakong, H. J. Kim, S. H. Kim, J. W. Namgoong, J. H. Park, J.-H. Ryu, B. Kim, M. J. Ko and J. P. Kim, *New J. Chem.*, 2012, **36**, 2025–2032.

16 M.-D. Zhang, H. Pan, X.-H. Ju, Y.-J. Ji, L. Qin, H.-G. Zheng and X.-F. Zhou, *Phys. Chem. Chem. Phys.*, 2012, **14**, 2809–2815.

17 S. Wang, J. Guo, L. He, H. Wang, J. Zhao and C. Lu, *Synth. Met.*, 2013, **168**, 1–8.

18 M. Liang and J. Chen, *Chem. Soc. Rev.*, 2013, **42**, 3453–3488.

19 D. P. Hagberg, T. Marinado, K. M. Karlsson, K. Nonomura, P. Qin, G. Boschloo, T. Brinck, A. Hagfeldt and L. Sun, *J. Org. Chem.*, 2007, **72**, 9550–9556.

20 L. Zhang, Y. Liu, Z. Wang, M. Liang, Z. Sun and S. Xue, *Tetrahedron*, 2010, **66**, 3318–3325.

21 D. P. Hagberg, X. Jiang, E. Gabrielsson, M. Linder, T. Marinado, T. Brinck, A. Hagfeldt and L. Sun, *J. Mater. Chem.*, 2009, **19**, 7232–7238.

22 Molecule **4b** has been previously reported. Initially the molecule was prepared by Park *et al.* and studied as a photocatalyst. No device data were given. More recently, during the preparation of this manuscript, Wang *et al.* (*Synthetic Metals*, 2013, **128**, 1–8) reported the characterization and device parameters of **4b**, but there are significant discrepancies between their characterization data and ours.

23 M. h. Chahma, J. B. Gilroy and R. G. Hicks, *J. Mater. Chem.*, 2007, **17**, 4768–4771.